

# 11

## Numerical methods

Until now, we have mostly considered magnetostatic problems that have analytic solutions. In practice, this has usually restricted our choice of problems to situations where one of the problem boundaries coincides with a coordinate system axis and to solutions that can be written as products of functions of a single coordinate. Frequently, more complicated problems can only be solved using numerical methods.[1] A number of commercial and freeware programs are available for solving magnetic problems. A lot of effort has been devoted to making many of these programs accurate, efficient, and user-friendly. If such a program is available and can address the problem under consideration, it is often the best choice to use it. However, there are occasions when new code must be written to solve a problem. It is also important to have some basic understanding about the methods involved in obtaining these solutions. In this chapter, we will examine three numerical methods that have been used for solving boundary value problems involving the Poisson equation: finite differences, finite elements, and integral equations. In each case, the analytical equation or its solution is approximated in some way that leads to a matrix equation for the unknown potential or field. We conclude the chapter with a discussion of inverse problems and optimization techniques.

### 11.1 Finite difference method

In the finite difference method, the continuous space of the problem domain is replaced with a grid of discrete points called *nodes*. [1] The grid, which is commonly rectangular or polar, must extend over the whole space of the problem. This usually requires grid points outside all conductors and iron, out to a point where the potential has some assumed value, typically zero. Symmetries in the configuration may be used to reduce the required grid size. For some problems, it may be necessary to use reduced grid spacing in regions where the field gradient is large or where high accuracy is required.

Unknown quantities are calculated at the nodes. Derivatives defined on the continuous domain of the physical problem are replaced with difference approximations defined in terms of the values of the unknown function at the nodes. For example, assume that  $u$  is an unknown function and that a one-dimensional problem space has been discretized with the grid spacing  $h = \Delta x$ . The Taylor series for the node at location  $x + h$  is

$$u(x + h) = u(x) + h \frac{\partial u}{\partial x} \Big|_x + \frac{h^2}{2!} \frac{\partial^2 u}{\partial x^2} \Big|_x + \mathcal{O}(h^3). \quad (11.1)$$

Ignoring second- and higher-order terms, the first derivative can be approximated in terms of the node values by

$$\frac{\partial u}{\partial x} \simeq \frac{u(x + h) - u(x)}{h}. \quad (11.2)$$

This is called the *forward difference* because it involves the next higher node than the node at  $x$ . Similarly taking  $h \rightarrow -h$ , we find the *backward difference* is

$$\frac{\partial u}{\partial x} \simeq \frac{u(x) - u(x - h)}{h}. \quad (11.3)$$

We can obtain an approximation for the derivative that is accurate through the  $h^2$  term in the Taylor series by calculating

$$u(x + h) - u(x - h) \simeq u + hu' + \frac{h^2}{2} u'' - u + hu' - \frac{h^2}{2} u''.$$

The *central difference* approximation for the first derivative is then

$$\frac{\partial u}{\partial x} \simeq \frac{u(x + h) - u(x - h)}{2h}. \quad (11.4)$$

We can approximate the second derivative from its definition as

$$\begin{aligned} \frac{\partial^2 u}{\partial x^2} &\simeq \frac{1}{h} \left[ \frac{u(x + h) - u(x)}{h} - \frac{u(x) - u(x - h)}{h} \right] \\ &= \frac{1}{h^2} [u(x + h) - 2u(x) + u(x - h)]. \end{aligned} \quad (11.5)$$

**Example 11.1:** one-dimensional Poisson equation

To illustrate the basic concepts of the finite difference method, let us consider the solution of the one-dimensional Poisson's equation

$$\frac{\partial^2 u}{\partial x^2} = f$$

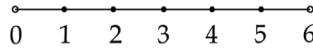


Figure 11.1 Nodes on a line.

in the greatly simplified situation shown in Figure 11.1. The line is discretized into 7 nodes. Let  $u$  refer to the unknown quantity, which we assume satisfies the Dirichlet boundary conditions  $u_0 = 0$  and  $u_6 = 0$ . Assume that the source function  $f$  has the value  $f_3 = v$  at the center of the line and is 0 otherwise. The values of  $u$  at the five interior nodes are the unknown quantities. Using Equation 11.5, each interior node satisfies the equation

$$u(x+h) - 2u(x) + u(x-h) = h^2 f.$$

We can write the equations for the five unknowns in the form of a matrix equation

$$Cu = g. \quad (11.6)$$

For the case here, we have

$$\begin{bmatrix} -2 & 1 & 0 & 0 & 0 \\ 1 & -2 & 1 & 0 & 0 \\ 0 & 1 & -2 & 1 & 0 \\ 0 & 0 & 1 & -2 & 1 \\ 0 & 0 & 0 & 1 & -2 \end{bmatrix} \begin{bmatrix} u_1 \\ u_2 \\ u_3 \\ u_4 \\ u_5 \end{bmatrix} = \begin{bmatrix} 0 \\ 0 \\ v \\ 0 \\ 0 \end{bmatrix},$$

which has the solution

$$u = \begin{bmatrix} -\frac{1}{2} h^2 v \\ -h^2 v \\ -\frac{3}{2} h^2 v \\ -h^2 v \\ -\frac{1}{2} h^2 v \end{bmatrix}.$$

For a square grid in two dimensions, let us designate the node under consideration as node 0 and its four nearest neighbors as nodes 1–4, as shown in Figure 11.2. We can write the Laplacian operator in terms of the values at the five nodes as [2]

$$\nabla^2 u \simeq \frac{1}{h^2} [u(x-h, y) + u(x+h, y) + u(x, y-h) + u(x, y+h) - 4u(x, y)]. \quad (11.7)$$

It is also possible to write a generalized version for the two-dimensional Laplacian where the distances from a given node to each of its nearest neighbors can be different. If  $h$  is the characteristic grid spacing, then [3]

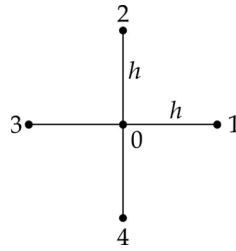


Figure 11.2 Node structure in two dimensions.

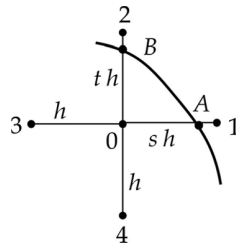


Figure 11.3 Node near a curved boundary.

$$\nabla^2 u \simeq \frac{2}{h^2} \left[ \frac{u_1}{p(p+r)} + \frac{u_2}{q(q+s)} + \frac{u_3}{r(p+r)} + \frac{u_4}{s(q+s)} - \left( \frac{1}{pr} + \frac{1}{qs} \right) u_0 \right], \quad (11.8)$$

where  $p, q, r, s$  are dimensionless scaling factors for the spacings from node 0 to its nearest neighbors. Using this expression for problems where the physical boundaries of conductors and iron are parallel to the  $x$  and  $y$  axes, it is possible to set up the equations for the interior nodes together with nodes coinciding with the boundaries. Higher-order difference equations for the Laplacian are also possible.[4]

A complication arises in setting up the node equations for nodes adjacent to boundaries that do not align exactly with the grid spacing, for example nodes next to circular boundaries in a rectangular grid. For Dirichlet boundary conditions, we can make use of the fact that we know the value of  $u(x, y)$  on the boundary. Consider a node 0 adjacent to the boundary shown in Figure 11.3. The two-dimensional Laplacian operator acting at  $u_0$  can be approximated as [5]

$$\nabla^2 u \simeq \frac{2}{h^2} \left[ \frac{u_A}{s(1+s)} + \frac{u_B}{t(1+t)} + \frac{u_3}{1+s} + \frac{u_4}{1+t} - \left( \frac{1}{s} + \frac{1}{t} \right) u_0 \right], \quad (11.9)$$

where  $s$  and  $t$  are dimensionless scale factors.

There are also complications in setting up the difference equations when the problem requires Neumann boundary conditions.[6] Here we will only consider the situation shown in Figure 11.4, which is a planar boundary in a square grid between

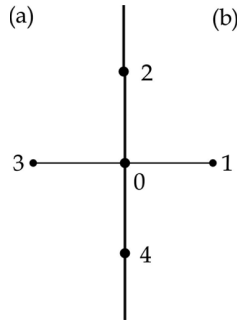


Figure 11.4 Boundary between regions with different permeabilities.

two regions (a) and (b) with different permeabilities. Let us consider an arbitrary point 0 along the boundary. Since point 0 is part of region a, the Laplace equation is

$$A_{a1} + A_2 + A_{a3} + A_4 - 4A_0 = 0, \tag{11.10}$$

where we use  $A$  for the unknown function here. For region a, node 1 is fictitious and must be eliminated from the final difference equation. Node 0 is also a part of region b, so we have

$$A_{b1} + A_2 + A_{b3} + A_4 - 4A_0 = 0, \tag{11.11}$$

where node 3 is fictitious in region b. The Neumann boundary condition at node 0 is

$$\frac{1}{\mu_a} \left( \frac{A_{a1} - A_{a3}}{2h} \right) = \frac{1}{\mu_b} \left( \frac{A_{b1} - A_{b3}}{2h} \right).$$

Substituting for  $A_{a1}$  from Equation 11.10 and  $A_{b3}$  from Equation 11.11, we find the difference equation at boundary point 0 is

$$4A_0 - \frac{2\mu_a}{\mu_a + \mu_b} A_{b1} - A_2 - \frac{2\mu_b}{\mu_a + \mu_b} A_{a3} - A_4 = 0. \tag{11.12}$$

If region b has infinite permeability, then the difference equation simplifies to

$$4A_0 - A_2 - 2A_{a3} - A_4 = 0. \tag{11.13}$$

Interpolation must be used when a value of some quantity  $u$  is required at a location away from one of the nodes. Suppose we want the value of the function  $u(x, y)$ , as shown for a rectangular grid in Figure 11.5. The simplest scheme for estimating the value of  $u$  is *bilinear interpolation*. We first determine which rectangle in the grid that the desired point is located in. Then defining the variables

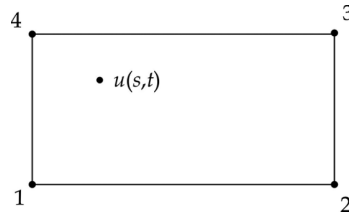


Figure 11.5 Bilinear interpolation.

$$s = \frac{x - x_1}{x_2 - x_1}$$

$$t = \frac{y - y_1}{y_2 - y_1},$$

we can approximate the value of  $u(x, y)$  as [7]

$$u(s, t) \simeq (1 - s)(1 - t)u_1 + s(1 - t)u_2 + stu_3 + (1 - s)tu_4. \quad (11.14)$$

This expression varies continuously in  $x$  and  $y$  and reduces correctly to the node values at the corners of the rectangle.

The discrepancy between the result from using the difference approximation and the exact result from solving the differential equation is known as the truncation error. The error can be estimated by examining the first term in the Taylor series that was neglected in deriving the difference formula under consideration. For a square mesh, the error on the second derivative goes like

$$\sim \frac{2h^2}{4!} \frac{\partial^4 u}{\partial x^4} \Big|_0.$$

The error is proportional to  $h^2$ , so one method of improving the accuracy in a finite difference calculation is to reduce the mesh spacing. We can monitor the improvement in accuracy by finding the maximum absolute value for the difference

$$e_{ij} = u_{ij}^{h_2} - u_{ij}^{h_1},$$

where the superscript refers to the mesh spacing used for the solution and  $(i, j)$  refers to nodes common to both mesh spacings. This approach is ultimately limited by the growth in the size of the coefficient matrix and by rounding errors in the numerical calculations. An alternative approach for increasing the accuracy of the calculation is to use higher-order difference equations.

The quality of a solution can be monitored by calculating the *residual* for each of the interior nodes. For a general node for the Poisson equation, the residual is defined as

$$R_{i,j} = 4 u_{i,j} - u_{i,j+1} - u_{i,j-1} - u_{i+1,j} - u_{i-1,j} - h^2 \mu_{i,j} J_{i,j}. \quad (11.15)$$

If the difference equation exactly satisfies Poisson's equation, the residual should be 0.

For problems using iteration algorithms, we can compute

$$e_{ij} = u_{ij}^n - u_{ij}^{n-1}$$

for the unknown function at the node  $(i,j)$ , where the superscript refers to the iteration number. For these methods, one can estimate the quality of the solution by calculating the difference at all the nodes. Let  $M$  refer to the absolute value of the largest difference in the mesh.

$$M = \max |e_{ij}|$$

For the 5-point Laplacian operator in Equation 11.7, the error  $\varepsilon$  between the exact solution of the difference equation and the approximate solution after  $n$  iterations is bounded by [8]

$$\varepsilon \leq \frac{M\rho^2}{4h^2}, \quad (11.16)$$

where  $\rho$  is the radius of the smallest circle that encompasses the entire field region.

In problems where iron saturation is a consideration, the permeability of the iron can be made a variable at each of the nodes in the iron regions.[9] The permeabilities are stored on a separate mesh. After each iteration of the potential, the field in the iron region is updated. A table of  $B$ - $\mu$  values can be used to relate the permeability to the field at the node. The mesh of permeability values is then updated using, for example, an under-relaxation algorithm.

## 11.2 Example solution using finite differences

As a simple example, let us consider a rectangular conductor with constant current density  $\mathbf{J}$  close to a sheet of iron with permeability  $\mu_r = 100$ , as shown in Figure 11.6.

Assume that the conductor and the sheet are uniform in the  $z$  direction, so that a two-dimensional analysis is justified. Assume that the figure is up-down symmetric, so that the  $x$  axis lies in a symmetry plane. We solve the problem using finite differences on a square  $200 \times 200$  mesh. For simplicity, we have chosen the boundaries of the conductor and the iron sheet to line up with node locations. The problem requires Dirichlet boundary conditions on the left, right, and top outer borders, where we set  $A_z = 0$ . Because of the up-down symmetry, the bottom border requires a Neumann boundary condition.

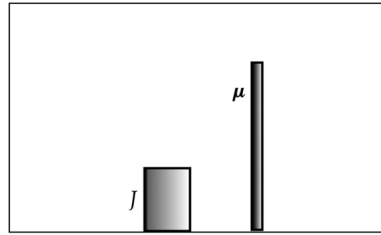


Figure 11.6 Conductor close to an iron sheet.

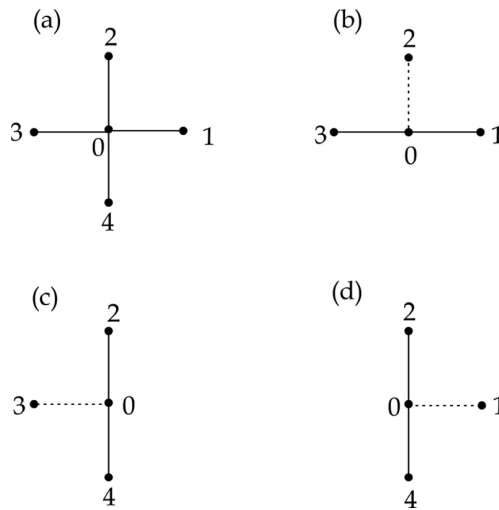


Figure 11.7 Finite difference node patterns.

In applying the Poisson equation here, four types of node patterns are required, as shown in Figure 11.7. In each case, node 0 refers to the node we are currently evaluating. For a general interior node where all the neighbor nodes are in the same region, we apply the pattern (a), which results in the relation

$$4A_0 = A_1 + A_2 + A_3 + A_4 + f, \quad (11.17)$$

where  $f = h^2\mu J$  for nodes inside the conductor and 0 otherwise. For nodes on the symmetry plane, pattern (b) gives

$$4A_0 = A_1 + 2A_2 + A_3 + f.$$

For the left side of the iron sheet, we can use Equation 11.12 for pattern (c) with  $\mu_a = 1$  and  $\mu_b = 100$ . For the right side of the sheet, we use Equation 11.12 for pattern (d) with  $\mu_a = 100$  and  $\mu_b = 1$ .



For problems with a very large number of unknown nodes, it is not practical to solve the matrix equation using direct methods. Instead iterative methods must be used. A common method is to use the Successive Overrelaxation (SOR) algorithm. [10, 11] Let us define  $A_{j,k}^n$  to be the value of the potential at the interior node at location  $(j, k)$  after  $n$  iterations. On the next iteration, we update the value of the potential according to the prescription

$$A_{j,k}^{n+1} = (1 - \alpha) A_{j,k}^n + \alpha A_{j,k}^*, \quad (11.18)$$

where  $\alpha$  is called the overrelaxation parameter. For efficient convergence, we need  $1 < \alpha < 2$ . The optimal value for  $\alpha$  is problem dependent, but the value  $\alpha \sim 1.7$ , which we use here, is typical. The quantity  $A_{j,k}^*$  is the solution for  $A_{j,k}$  from the appropriate nodal solution of Poisson's equation. For example, using Equation 11.17 for a general node, the SOR relation is

$$A_{j,k}^{n+1} = (1 - \alpha) A_{j,k}^n + \frac{\alpha}{4} \left[ A_{j-1,k}^{n+1} + A_{j+1,k}^n + A_{j,k-1}^{n+1} + A_{j,k+1}^n + f_{j,k} \right].$$

Thus the updated value of the potential has two contributions. The first term is an adjustable fraction of its value on the previous iteration. The second term is a fraction of the Poisson equation residual at the node, calculated from the values of the potential at the neighbor nodes. Note that the calculation of the residual uses values for two nodes that have already been updated for a given iteration and values for two nodes from the previous iteration. The iterations continue until

$$\max \left| \frac{A_{j,k}^{n+1} - A_{j,k}^n}{A_{j,k}^n} \right| \leq \tau$$

over all the interior nodes.<sup>1</sup> The tolerance  $\tau = 10^{-5}$  was used in this example. This criterion was satisfied after 7,511 iterations.

The magnetic field was calculated at the center of every square formed by four neighbor nodes, as shown in Figure 11.8.

$$B_x = \partial_y A_z = \frac{1}{2h} (-A_1 + A_2 + A_3 - A_4)$$

$$B_y = -\partial_x A_z = -\frac{1}{2h} (A_1 + A_2 - A_3 - A_4).$$

The results of the calculations for the magnetic field are shown in Figure 11.9.

<sup>1</sup> Or just the difference in values if the potential is 0.

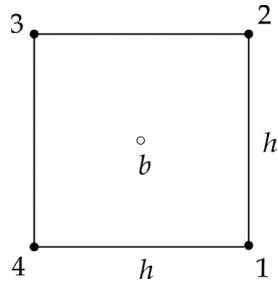


Figure 11.8 Magnetic field calculation.

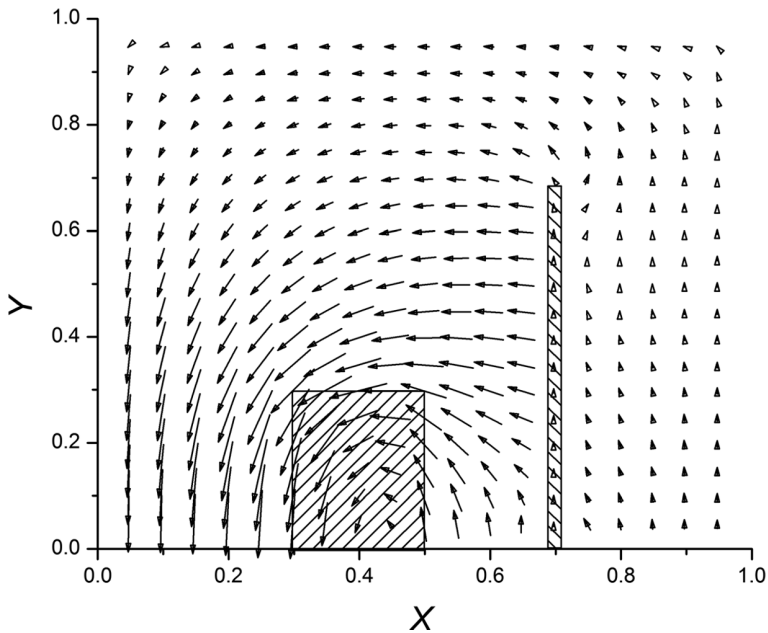


Figure 11.9 Magnetic field pattern for the example finite difference problem.

### 11.3 Finite element method

In the finite element method, the problem space is completely subdivided into a set of subregions called finite elements.[1, 12] The potential in each element is represented by an interpolation function that is defined in terms of the potential values at the nodes of the element. The Poisson equation and its boundary conditions can be formulated in terms of energy functionals. The minimization of this functional generates a set of algebraic equations that can be solved directly or through iterative techniques. The method is quite flexible since there is considerable freedom in choosing element shapes to match boundary and interface geometries.

For simplicity, we restrict our discussion here to two-dimensional problems. The nonlinear Poisson equation can be written in the form

$$\frac{\partial}{\partial x} \left( \gamma \frac{\partial A}{\partial x} \right) + \frac{\partial}{\partial y} \left( \gamma \frac{\partial A}{\partial y} \right) = -J,$$

where  $\gamma$  is the reluctivity and  $A$  and  $J$  only have nonvanishing components in the  $z$  direction. This differential equation can be expressed in terms of the energy functional [13]

$$\mathcal{F} = \iint \left[ \int_0^B \gamma b \, db - JA \right] dx \, dy - \oint A \frac{\partial A}{\partial n} \, dl, \quad (11.19)$$

where  $b$  is the magnitude of the magnetic field.

$$b = \sqrt{\left( \frac{\partial A}{\partial x} \right)^2 + \left( \frac{\partial A}{\partial y} \right)^2}. \quad (11.20)$$

The line integral in Equation 11.19 vanishes since we require that the potential satisfy either Dirichlet or Neumann boundary conditions everywhere on the boundary. If the reluctivity is constant over an element, we can perform the integration over  $b$  to get the simplified energy functional

$$\mathcal{F} = \iint \left\{ \frac{\gamma}{2} \left[ \left( \frac{\partial A}{\partial x} \right)^2 + \left( \frac{\partial A}{\partial y} \right)^2 \right] - JA \right\} dx \, dy. \quad (11.21)$$

The simplest two-dimensional finite element is a triangle, as shown in Figure 11.10. We assume the potential varies linearly inside the element.

$$A = c_1 + c_2 x + c_3 y. \quad (11.22)$$

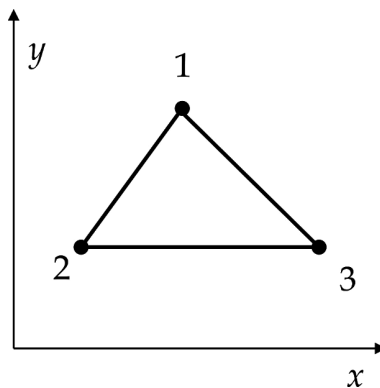


Figure 11.10 Triangular finite element.

If we write this expression for each of the three nodes, we have three equations that can be solved for the three unknown coefficients  $c_i$  in terms of the potentials and coordinates at the nodes. Substituting the result back into Equation 11.22, we find

$$\begin{aligned}
 A = & A_1 \left[ \frac{(x_2 y_3 - x_3 y_2) + (y_2 - y_3)x + (x_3 - x_2)y}{2S} \right] \\
 & + A_2 \left[ \frac{(x_3 y_1 - x_1 y_3) + (y_3 - y_1)x + (x_1 - x_3)y}{2S} \right] \\
 & + A_3 \left[ \frac{(x_1 y_2 - x_2 y_1) + (y_1 - y_2)x + (x_2 - x_1)y}{2S} \right],
 \end{aligned} \tag{11.23}$$

where  $S$  is the area of the triangle.

$$S = \frac{1}{2}[(x_2 y_3 - x_3 y_2) + (y_2 - y_3)x_1 + (x_3 - x_2)y_1] \tag{11.24}$$

The coefficients of the node potentials in this equation are known as *shape functions*,  $\zeta_i$ . [14] Thus we can also write the interpolation function for the potential as

$$A = \zeta_1 A_1 + \zeta_2 A_2 + \zeta_3 A_3. \tag{11.25}$$

The shape function  $\zeta_1$  has the properties that

$$\begin{aligned}
 \zeta_1(x_1, y_1) &= 1 \\
 \zeta_1(x_2, y_2) &= 0 \\
 \zeta_1(x_3, y_3) &= 0
 \end{aligned}$$

and similarly for  $\zeta_2$  and  $\zeta_3$ .

In order to evaluate the simplified energy functional in Equation 11.21, we need the derivatives of  $A$  from Equation 11.23.

$$\begin{aligned}
 \frac{\partial A}{\partial x} &= \frac{(y_2 - y_3)A_1 + (y_3 - y_1)A_2 + (y_1 - y_2)A_3}{2S} \\
 \frac{\partial A}{\partial y} &= \frac{(x_3 - x_2)A_1 + (x_1 - x_3)A_2 + (x_2 - x_1)A_3}{2S}
 \end{aligned} \tag{11.26}$$

Substituting into Equation 11.21, we get

$$\begin{aligned}
 \mathcal{F} = & \frac{\gamma}{2} \iint \left\{ \frac{[(y_2 - y_3)A_1 + (y_3 - y_1)A_2 + (y_1 - y_2)A_3]^2}{4S^2} \right. \\
 & \left. + \frac{[(x_3 - x_2)A_1 + (x_1 - x_3)A_2 + (x_2 - x_1)A_3]^2}{4S^2} \right\} dx dy \\
 & - \iint JA dx dy.
 \end{aligned}$$

The solution of the field equations is equivalent to finding a function  $A$  that minimizes this energy functional.[15] The potentials at the three nodes may be considered to be the parameters of the functional  $\mathcal{F}$  for a given element. Thus we require that

$$\begin{aligned} \frac{\partial \mathcal{F}}{\partial A_1} = \frac{\gamma}{2} \iint \left\{ \frac{2[(y_2 - y_3)A_1 + (y_3 - y_1)A_2 + (y_1 - y_2)A_3](y_2 - y_3)}{4S^2} \right. \\ \left. + \frac{2[(x_3 - x_2)A_1 + (x_1 - x_3)A_2 + (x_2 - x_1)A_3](x_3 - x_2)}{4S^2} \right\} dx dy \\ - \iint J \frac{\partial A}{\partial A_1} dx dy = 0 \end{aligned}$$

with analogous expressions for the derivatives with respect to  $A_2$  and  $A_3$ . The integrand for the first integral is independent of  $x$  and  $y$  and the integrand for the second integral may be evaluated using Equation 11.23. Thus we have

$$\begin{aligned} \frac{\partial \mathcal{F}}{\partial A_1} = \frac{\gamma}{4S} \left[ (y_2 - y_3)^2 A_1 + (y_3 - y_1)(y_2 - y_3)A_2 + (y_1 - y_2)(y_2 - y_3)A_3 \right] \\ + \frac{\gamma}{4S} \left[ (x_3 - x_2)^2 A_1 + (x_1 - x_3)(x_3 - x_2)A_2 + (x_2 - x_1)(x_3 - x_2)A_3 \right] \\ - \iint J \frac{[(x_2 y_3 - x_3 y_2) + (y_2 - y_3)x + (x_3 - x_2)y]}{2S} dx dy = 0 \end{aligned}$$

with analogous expressions for the derivatives with respect to  $A_2$  and  $A_3$ . For elements containing current, the second integral can be evaluated by assuming that  $J$  is constant and that  $x$  and  $y$  are evaluated at the centroid of the triangle.

$$\begin{aligned} x_c &= \frac{x_1 + x_2 + x_3}{3} \\ y_c &= \frac{y_1 + y_2 + y_3}{3}. \end{aligned}$$

In this case, the numerator in the last term is  $2S/3$ , so the integral has the value  $JS/3$ . Thus minimization of the functional over the triangular element leads to the matrix equation

$$\frac{\gamma}{4S} \begin{bmatrix} C_{11} & C_{12} & C_{13} \\ C_{21} & C_{22} & C_{23} \\ C_{31} & C_{32} & C_{33} \end{bmatrix} \begin{bmatrix} A_1 \\ A_2 \\ A_3 \end{bmatrix} = \frac{JS}{3} \begin{bmatrix} 1 \\ 1 \\ 1 \end{bmatrix}. \quad (11.27)$$

The coefficient matrix  $C$  is symmetric with six unique elements.

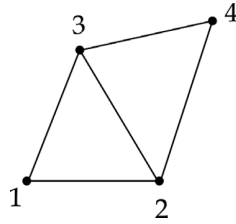


Figure 11.11 Two neighboring 2D elements.

$$\begin{aligned}
 C_{11} &= (y_2 - y_3)^2 + (x_3 - x_2)^2 \\
 C_{12} &= (y_3 - y_1)(y_2 - y_3) + (x_1 - x_3)(x_3 - x_2) \\
 C_{13} &= (y_1 - y_2)(y_2 - y_3) + (x_2 - x_1)(x_3 - x_2) \\
 C_{22} &= (y_3 - y_1)^2 + (x_1 - x_3)^2 \\
 C_{23} &= (y_3 - y_1)(y_1 - y_2) + (x_1 - x_3)(x_2 - x_1) \\
 C_{33} &= (y_1 - y_2)^2 + (x_2 - x_1)^2.
 \end{aligned} \tag{11.28}$$

Each triangular element introduces an analogous set of equations. However, if  $N$  is the total number of elements, the number of unknown potentials is less than  $3N$  because all of the elements share boundaries with neighbor triangles. For example, if we consider the two elements shown in Figure 11.11, the first element introduces three unknown potentials while the second element only adds one more. The resulting set of equations can be solved for the potentials using direct or iterative methods.

Setting up a realistic finite element problem involves a great deal of careful bookkeeping and computations.[13, 15] The problem space must be completely covered by the set of finite elements. The elements and nodes must be indexed and the association of each element with its corresponding nodes, current, and permeability must be clearly established. The boundary conditions must be imposed on the appropriate subset of the nodes. The coefficients for Equation 11.27 must be determined and an appropriate method used for solving the resulting system of equations. Additional iterative techniques must be applied if the problem contains saturable iron.

#### 11.4 Integral equation method

Thus far we have discussed numerical methods for solving the Poisson differential equation directly and for solving the potentials by minimizing the energy functional for the magnetostatic field. Here we examine a third approach where the unknown potentials or sources of the field are expressed in terms of an integral

equation. A major advantage of the integral equation method over methods based on the solution of a differential equation is that the mesh only needs to encompass the iron region (and possibly the conductor region if the current density is not uniform).[16, 17] The boundary condition at infinity follows naturally and does not have to be imposed at the edge of a mesh. An important disadvantage is that the resulting matrix equation is dense, so the solution time grows rapidly as the number of elements is increased. Also the flux density computed near the iron elements can be strongly affected by the discretization. There are many ways to formulate a solution of Poisson's equation using integral equations.[17, 18, 19] In addition, it is also possible to formulate procedures which combine differential and integral equation techniques.[20]

We describe here an integral equation approach that uses the magnetization of iron elements as the unknown function.<sup>2</sup> Recall that the magnetization is related to the magnetic field intensity by

$$\vec{M} = \frac{\vec{B}}{\mu_0} - \vec{H} = \chi(H) \vec{H}, \quad (11.29)$$

where  $\chi$  is the susceptibility. The field intensity has contributions from both conductor currents and from the magnetization in the iron. The total field intensity is

$$\vec{H} = \vec{H}_c + \vec{H}_m,$$

so the magnetization is given by

$$\vec{M} = \chi (\vec{H}_c + \vec{H}_m).$$

The contribution  $H_c$  can be calculated for simple conductor configurations using the complex variable techniques given in Chapter 5 or directly from the Biot-Savart law

$$\vec{H}_c(\vec{r}) = \frac{1}{4\pi} \int \frac{\vec{J}(\vec{r}') \times \vec{R}}{R^3} dV', \quad (11.30)$$

where  $\vec{R} = \vec{r} - \vec{r}'$ . Using Equation 3.32, the field due to the magnetization is

$$\vec{H}_m(\vec{r}) = -\frac{1}{4\pi} \nabla \int \vec{M}(\vec{r}') \cdot \frac{\vec{R}}{R^3} dV'. \quad (11.31)$$

<sup>2</sup> This procedure was adopted by a group at the Rutherford High Energy Laboratory in the development of the GFUN program.

Break the iron region into  $N$  elements and assume the magnetization is constant over the area of each element. The magnetization at some element  $i$  will depend on the field at  $i$  due to the conductors and on the field at  $i$  due to the magnetization from all the elements. Thus we have

$$\vec{M}_i = \chi_i \left[ \vec{H}_{ci} - \frac{1}{4\pi} \nabla_i \int \sum_{j=1}^N \vec{M}_j \cdot \frac{\vec{R}_{ij}}{R_{ij}^3} dV_j \right]. \quad (11.32)$$

We define the contribution to the field at element  $i$  due to the magnetization at element  $j$  in terms of the coupling constants

$$G_{ij} = -\frac{1}{4\pi} \nabla_i \int \hat{M}_j \cdot \frac{\vec{R}_{ij}}{R_{ij}^3} dV_j. \quad (11.33)$$

It is important to note that the components of  $G$  depends on the directions of the unit vectors used to define  $M$ , but do not depend on the magnitude of  $M$ . We can then rewrite Equation 11.32 as

$$\vec{M}_i = \chi_i \left[ \vec{H}_{ci} + \sum_{j=1}^N G_{ij} \vec{M}_j \right].$$

Rearranging this equation, we have

$$\frac{\vec{M}_i}{\chi_i} - \sum_{j=1}^N G_{ij} \vec{M}_j = \vec{H}_{ci},$$

which can be written in the standard matrix equation form [17]

$$\sum_{j=1}^N \left( \frac{\delta_{ij}}{\chi_j} - G_{ij} \right) \vec{M}_j = \vec{H}_{ci}. \quad (11.34)$$

This is a set of algebraic equations for the  $N$  unknown magnetization elements. The number of unknowns is  $2N$  for two-dimensional problems and  $3N$  for three dimensions. The field components due to the conductors at each iron element can be calculated directly, so the right-hand side of Equation 11.34 is known. However, the problem is generally nonlinear because  $\chi$  depends on the field due to the unknown magnetizations.

Returning to the definition of the coupling constant in Equation 11.33, we know from the vector identity B.2 that the gradient of the scalar product can be expanded as



$$\begin{aligned} \nabla_i \left( \hat{M}_j \cdot \frac{\vec{R}_{ij}}{R_{ij}^3} \right) &= \hat{M}_j \times \left[ \nabla_i \times \left( \frac{\vec{R}_{ij}}{R_{ij}^3} \right) \right] + \frac{\vec{R}_{ij}}{R_{ij}^3} \times (\nabla_i \times \hat{M}_j) + (\hat{M}_j \cdot \nabla_i) \left( \frac{\vec{R}_{ij}}{R_{ij}^3} \right) \\ &\quad + \left[ \frac{\vec{R}_{ij}}{R_{ij}^3} \cdot \nabla_i \right] \hat{M}_j. \end{aligned}$$

Two of the terms vanish because the derivative in field coordinates acts on the unit vector along the magnetization in source coordinates. Another term vanishes because of the curl operator acting on the linear vector  $R$ . Thus only the third term on the right-hand side remains. Writing this out in terms of components, we have

$$\begin{aligned} &(\hat{M}_j \cdot \nabla_i) \left( \frac{\vec{R}_{ij}}{R_{ij}^3} \right) \\ &= [\hat{M}_{jx} \partial_{ix} + \hat{M}_{jy} \partial_{iy} + \hat{M}_{jz} \partial_{iz}] \left[ \frac{(x_i - x_j)\hat{x} + (y_i - y_j)\hat{y} + (z_i - z_j)\hat{z}}{\{(x_i - x_j)^2 + (y_i - y_j)^2 + (z_i - z_j)^2\}^{3/2}} \right] \\ &= \frac{\hat{M}_{jx}}{R_{ij}^5} [R_{ij}^2 \hat{x} - 3(x_i - x_j) \vec{R}] + \frac{\hat{M}_{jy}}{R_{ij}^5} [R_{ij}^2 \hat{y} - 3(y_i - y_j) \vec{R}] + \frac{\hat{M}_{jz}}{R_{ij}^5} [R_{ij}^2 \hat{z} - 3(z_i - z_j) \vec{R}]. \end{aligned}$$

After inserting this expression into Equation 11.33, we can identify the three-dimensional coupling constants

$$\begin{aligned} G_{ix,jx} &= -\frac{1}{4\pi} \int \frac{R_{ij}^2 - 3(x_i - x_j)^2}{R_{ij}^5} dV_j \\ G_{ix,jy} &= -\frac{1}{4\pi} \int \frac{-3(x_i - x_j)(y_i - y_j)}{R_{ij}^5} dV_j \end{aligned}$$

and similarly for the other components.[21, 22] The  $G$  coupling matrix is symmetric. There are constraints on the sum of the diagonal elements.[21]

$$G_{ix,jx} + G_{iy,jy} + G_{iz,jz} = \begin{cases} 0 & \text{if } i \neq j \\ -1 & \text{if } i = j \end{cases}$$

In two dimensions,  $M_j$  is uniform along  $z$ , the field observation point has  $z_i = 0$ , and  $\nabla_i$  and  $M_j$  only have  $x$  and  $y$  components. We find the two-dimensional coupling constants by integrating the three-dimensional couplings over  $z$

$$G_{ij} = -\frac{1}{4\pi} \iint (\hat{M}_j \cdot \nabla_i) \left( \frac{\vec{R}_{ij}}{R_{ij}^3} \right) dz_j dS_j,$$

where  $dS_j$  is the two-dimensional area element. This can be written in the form

$$G_{ij} = -\frac{1}{4\pi} \int [\hat{M}_{jx} \mathbb{I}_1 + \hat{M}_{jy} \mathbb{I}_2] dS_j, \quad (11.35)$$

where

$$\mathbb{I}_1 = \int_{-\infty}^{\infty} \frac{R_{ij}^2 \hat{x} - 3(x_i - x_j)[(x_i - x_j)\hat{x} + (y_i - y_j)\hat{y} - z_j\hat{z}]}{R_{ij}^5} dz_j$$

and

$$\mathbb{I}_2 = \int_{-\infty}^{\infty} \frac{R_{ij}^2 \hat{y} - 3(y_i - y_j)[(x_i - x_j)\hat{x} + (y_i - y_j)\hat{y} - z_j\hat{z}]}{R_{ij}^5} dz_j.$$

Let  $r_{ij}$  be the distance between the observation point and the centroid of the iron element in the  $x$ - $y$  plane. Then the integral  $\mathbb{I}_1$  can be broken into the three simpler integrals<sup>3</sup>

$$\begin{aligned} \int_{-\infty}^{\infty} \frac{dz_j}{\{r_{ij}^2 + z_j^2\}^{3/2}} &= \frac{2}{r_{ij}^2} \\ \int_{-\infty}^{\infty} \frac{dz_j}{\{r_{ij}^2 + z_j^2\}^{5/2}} &= \frac{2}{3r_{ij}^4} \\ \int_{-\infty}^{\infty} \frac{z_j}{\{r_{ij}^2 + z_j^2\}^{5/2}} dz_j &= 0 \end{aligned}$$

with the result that

$$\begin{aligned} \mathbb{I}_1 &= \frac{2}{r_{ij}^2} \hat{x} - \frac{4(x_i - x_j)}{r_{ij}^4} \vec{r}_{ij} \\ \mathbb{I}_2 &= \frac{2}{r_{ij}^2} \hat{y} - \frac{4(y_i - y_j)}{r_{ij}^4} \vec{r}_{ij}. \end{aligned}$$

Inserting these results into Equation 11.35, we find the two-dimensional coupling constants are the dimensionless, geometric factors

<sup>3</sup> GR 2.271.5, 2.263.3, 2.271.7.

$$\begin{aligned}
 G_{ix,jx} &= \frac{1}{2\pi} \int \frac{(x_i - x_j)^2 - (y_i - y_j)^2}{r_{ij}^4} dS_j \\
 G_{ix,jy} = G_{iy,jx} &= \frac{1}{2\pi} \int \frac{2(x_i - x_j)(y_i - y_j)}{r_{ij}^4} dS_j \\
 G_{iy,jy} &= \frac{1}{2\pi} \int \frac{(y_i - y_j)^2 - (x_i - x_j)^2}{r_{ij}^4} dS_j.
 \end{aligned} \tag{11.36}$$

There are also constraints on the sum of the two-dimensional diagonal elements.[21]

$$G_{ix,jx} + G_{iy,jy} = \begin{cases} 0 & \text{if } i \neq j \\ -1 & \text{if } i = j \end{cases}$$

Once we know the coupling constants  $G$ , we can solve Equation 11.34 to find the magnetization in each of the iron elements. Then the field at any position can be found from the sum of the fields due to all the current elements together with the sum of all the fields due to the iron magnetizations. In applications where saturation in the iron is important, the permeability of all the iron elements must be recomputed using the magnetizations and a  $\mu$ - $H$  table for the iron material. The process is then iterated until the maximum change in permeability in any element is less than some tolerance value.

**Example 11.2:** setting up the integral equations for a dipole configuration

We will illustrate the two-dimensional integral equation algorithm by considering a simple example of currents and iron blocks arranged in a dipole configuration. Once the current and iron magnetization has been determined in the first quadrant, the dipole symmetry constrains the geometry and polarity of the currents and magnetizations in the other quadrants, as illustrated in Figure 11.12. The currents have polarities  $\{I, -I, -I, I\}$  in the four quadrants. If we let  $(M_x^{(1)}, M_y^{(1)})$  refer to the magnetization of an iron element in the first quadrant, then the dipole symmetry requires that

$$\begin{aligned}
 M_y^{(2)} &= M_y^{(3)} = M_y^{(4)} = M_y^{(1)} \\
 M_x^{(2)} &= M_x^{(4)} = -M_x^{(1)} \\
 M_x^{(3)} &= M_x^{(1)},
 \end{aligned}$$

where the numeral superscripts refer to the quadrants. Making use of the dipole symmetry allows us to treat only the magnetization components in the first quadrant as unknowns. This can be important in problems with large numbers of iron elements since it reduces the size of the matrix equation by a factor of four.

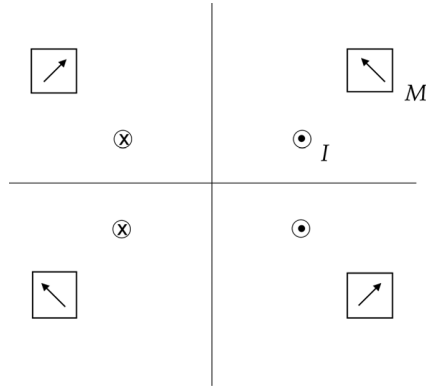


Figure 11.12 Dipole configuration of a current and iron magnetization.

Assume, for example, that there are two iron elements in the first quadrant. We can find the right-hand side of Equation 11.34 using the techniques in Chapters 4 and 5. We evaluate the field at the centroids of each of the iron elements. The magnetization has a constant magnitude and direction in each element. The coupling constants for the field due to the magnetizations can be found from Equation 5.72.

$$H^*(z_o) = \frac{M}{4\pi i} \oint \frac{dz^*}{z - z_o}.$$

We can determine the coupling constants  $G_{xx}$  and  $G_{yx}$  by evaluating  $H^*$  with  $M = 1$  and the coupling constants  $G_{xy}$  and  $G_{yy}$  by evaluating  $H^*$  with  $M = i$ .

The field components due to the magnetization in each iron element can be found from

$$\begin{aligned} H_{mx}^* &= G_{xx} M_x + G_{xy} M_y \\ H_{my}^* &= G_{yx} M_x + G_{yy} M_y. \end{aligned} \quad (11.37)$$

This gives the field anywhere outside the iron block. However, when the observation point is inside the block, the numerical procedure must ensure that  $H$  and  $M$  point in opposite directions, as they must inside a magnetic material. For the dipole configuration, we define the matrix coefficients  $C$  as sums over the coupling constants in the four quadrants. For example,

$$C_{i x j x} = G_{xx}^{(1)} - G_{xx}^{(2)} + G_{xx}^{(3)} - G_{xx}^{(4)},$$

where the minus signs take into account the reversal in the sign of  $M_x$  in the second and fourth quadrants. The other three coefficients are similarly defined. The matrix Equation 11.34 can be written for the case of two iron elements as

$$\begin{aligned}
(s_1 - C_{1x1x})M_{1x} - C_{1x1y}M_{1y} - C_{1x2x}M_{2x} - C_{1x2y}M_{2y} &= H_{c1x} \\
-C_{1y1x}M_{1x} + (s_1 - C_{1y1y})M_{1y} - C_{1y2x}M_{2x} - C_{1y2y}M_{2y} &= H_{c1y} \\
-C_{2x1x}M_{1x} - C_{2x1y}M_{1y} + (s_2 - C_{2x2x})M_{2x} - C_{2x2y}M_{2y} &= H_{c2x} \\
-C_{2y1x}M_{1x} - C_{2y1y}M_{1y} - C_{2y2x}M_{2x} + (s_2 - C_{2y2y})M_{2y} &= H_{c2y},
\end{aligned}$$

where  $s_i = 1/(\mu_{ri} - 1)$  and the numeral subscripts refer to the two iron elements in the first quadrant.

After solving the matrix equation,  $M$  is known for all the iron blocks. The contribution of the iron to the field at any location can be found using Equation 11.37, where  $G$  is now evaluated for the desired field point.

### 11.5 The POISSON code

We have shown results from the POISSON code<sup>4</sup> a number of times previously in this book. POISSON is one of the earliest examples of a finite element program. We give a brief description here of the method used in the code for solving the two-dimensional Poisson equation.[23, 24] The user defines the boundaries and properties of the physical regions in the problem, together with the boundary conditions at the borders of the problem space. The program then automatically sets up an irregular triangular mesh where every interior node is surrounded by six triangles. All boundaries and interfaces between regions lie on mesh lines. The current density is assumed to be constant in each triangle in a conductor region and the permeability is assumed to be constant in each triangle in an iron region.

The code does not solve the Poisson equation directly. Instead, the solution algorithm makes use of the Ampère law

$$\oint \vec{H} \cdot d\vec{l} = \int \vec{J} \cdot \hat{n} dS.$$

Allowing for saturation in the iron, this can be written as

$$\oint \gamma(B) \vec{B} \cdot d\vec{l} = \mu_0 \int \vec{J} \cdot \hat{n} dS,$$

where  $\gamma$  is the reluctivity. The vector potential is assumed to only have a  $z$  component and to satisfy  $\nabla \cdot \vec{A} = 0$ . Expressing  $B$  in terms of the vector potential, we get

<sup>4</sup> <http://laacg.lanl.gov/laacg/services>

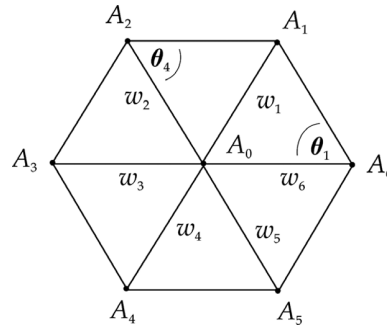


Figure 11.13 Relation among nodes in the POISSON algorithm.

$$\oint \gamma(B) \left[ \frac{\partial A}{\partial y} \hat{x} - \frac{\partial A}{\partial x} \hat{y} \right] \cdot d\vec{l} = \mu_0 \int \vec{J} \cdot \hat{n} dS.$$

The contour around each mesh point follows a twelve-sided path through the interior of the six surrounding triangles. After a lengthy calculation,[24] a difference equation for the potential at node 0 can be derived in terms of the potentials at the six neighbor nodes as

$$A_0 = \frac{\sum_{i=1}^6 A_i w_i + \frac{\mu_0}{3} \sum_{i=1}^6 J_i S_i}{\sum_{i=1}^6 w_i}.$$

In this equation, \$S\_i\$ is the area of the triangle. The \$w\_i\$ are coupling coefficients that involve the parameters of the triangles on adjacent sides of the line connecting \$A\_0\$ to neighboring node \$i\$. Looking at the diagram in Figure 11.13,

$$w_1 = \frac{1}{2}(\gamma_1 \cot \theta_1 + \gamma_2 \cot \theta_4)$$

with similar expressions for the other five couplings.

The vector potential varies linearly inside any triangle. As a result, the magnetic field is constant over the area of the triangle. Values for the potential are updated using the successive over-relaxation algorithm. The new values of the field are then used to estimate new values for \$\gamma\$ and for the couplings \$w\$. An under-relaxation algorithm is used to update the final values of the couplings for each iteration

$$w_i^{n+1} = (1 - \alpha)w_i^n + \alpha w_i^{new},$$

where the relaxation parameter satisfies \$0 < \alpha < 1\$.

As an illustration of using POISSON, we return to the simple problem discussed in Section 11.2. The input commands to define the problem are shown in

Table 11.1 *POISSON* input commands for the example problem

---



---

<b>Example: rectangular conductor near iron sheet</b>	
&reg kprob=0,	! Poisson or Pandira problem
icylin=0,	! rectangular coordinates
mode=-1,	! iron has fixed finite permeability
fixgam=0.01,	! reluctivity
dx=0.3,dy=0.3,	! mesh size intervals
nbslo=1,	! Neumann boundary condition on lower edge
nbsup=0,	! Dirichlet boundary condition on upper edge
nbslf=0,	! Dirichlet boundary condition on left edge
nbsrt=0 &	! Dirichlet boundary condition on right edge
&po x=0.0,y=0.0 &	! problem domain
&po x=100.,y=0.0 &	
&po x=100.0,y=100.0 &	
&po x=0.0,y=100.0 &	
&po x=0.0,y=0.0 &	
&reg mat=1,cur=19500. &	! conductor
&po x=30.0,y=0.0 &	
&po x=50.0,y=0. &	
&po x=50.0,y=30. &	
&po x=30.0,y=30.0 &	
&po x=30.0,y=0.0 &	
&reg mat=2 &	! iron sheet
&po x=70.0,y=0.0 &	
&po x=72.0,y=0.0 &	
&po x=72.,y=70.0 &	
&po x=70.,y=70.0 &	
&po x=70.0,y=0.0 &	

---



---

Table 11.1. The first REG command defines the problem domain and specifies the mesh size and the boundary conditions. The PO commands define points around the boundary of regions. The second region defines the conductor and specifies the current. The third region defines the iron sheet. POISSON sets up a triangular mesh using this information and then solves the Poisson equation using the SOR algorithm. For this example, the program used 112,896 mesh points, converged in 1,160 iterations, and had an average residual of  $5 \times 10^{-7}$ . The resulting field distribution, shown in Figure 11.14, agrees qualitatively well with the finite difference result in Figure 11.9. The shielding effects of the iron sheet are clearly apparent in the figure.

## 11.6 Inverse problems and optimization

We have previously defined the inverse problem as finding a current distribution that generates a specified magnetic field configuration. We discussed several problems of this type in Chapter 8. The solution of inverse problems is simplified

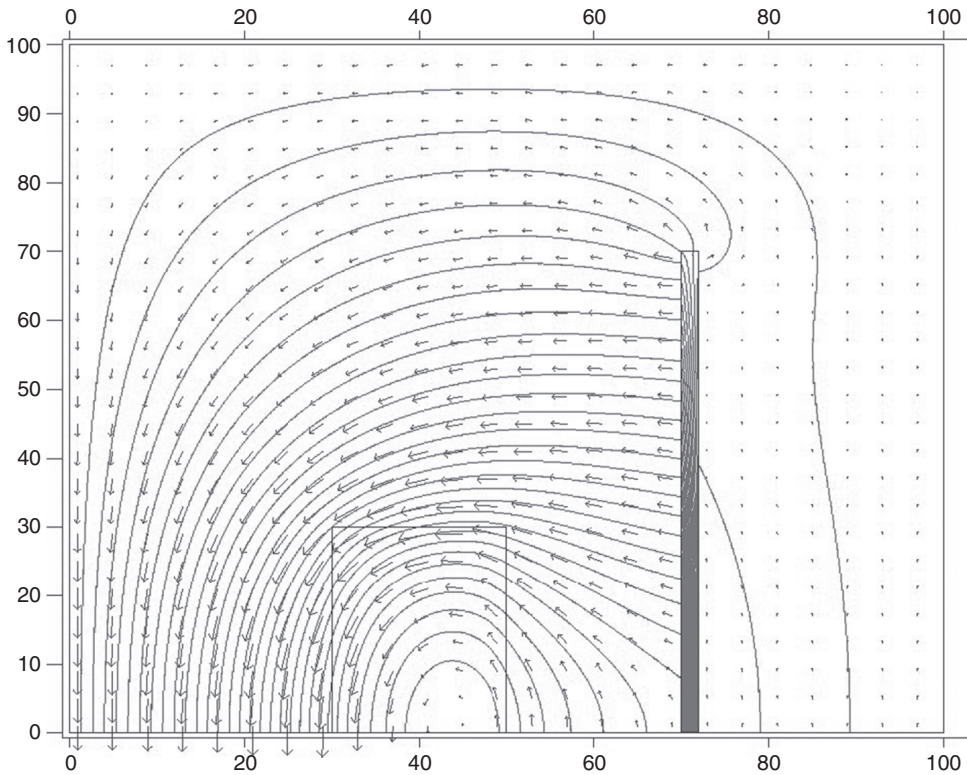


Figure 11.14 Field distribution for the example problem.

by constraining the coil geometry. For example, by specifying that the unknown currents lie on a cylindrical current sheet, it is possible to use Fourier-Bessel transforms to find the azimuthal and longitudinal current components that produce a specified target field inside a magnet aperture.[25] Another interesting approach used a numerical variational process to modify the contours of a uniform current density block conductor.[26] The target field was expressed in terms of a multipole expansion of the transverse field in the aperture. Higher-order multipoles were minimized by varying the geometry of the outer boundary of initial circular or elliptical current blocks.

A powerful technique for solving inverse problems is to make use of numerical optimization methods. Let us consider in more detail the numerical solution for two interesting inverse problems. As the first example, assume we have a solenoid channel with a constant axial field  $B_1$  and that we need to design an interface region to a second solenoid channel with constant axial field  $B_2$ . Assume the interface has length  $L$  measured from the center of the last magnet in the first channel to the center of the first magnet of the second channel. Assume in addition that the



transition region and second channel have to accept the full magnetic flux present in the first channel. Then the desired field profile in the interface region must satisfy the four constraints

$$\begin{aligned} B_z(0) &= B_1 \\ B_z(L) &= B_2 \\ \frac{dB_z}{dz}(0) &= 0 \\ \frac{dB_z}{dz}(L) &= 0. \end{aligned}$$

A model field profile that satisfies these constraints is

$$B_z(z) = \frac{B_1}{1 + c z^2 + d z^3}, \quad (11.38)$$

where

$$\begin{aligned} c &= \frac{3 (B_1 - B_2)}{B_2 L^2} \\ d &= -\frac{2 (B_1 - B_2)}{B_2 L^3}. \end{aligned}$$

If  $r_1$  is the inner radius of the coils in the first channel, then the requirement for constant flux puts an additional constraint on the allowed inner radius of the downstream coils.

$$r(z) \geq r_1 \sqrt{\frac{B_1}{B_z(z)}}.$$

For example, let the coil  $C_1$  be the last solenoid in a 10 T channel with a fixed inner radius of 10 cm and coil  $C_{14}$  be the first solenoid in a 2 T channel. Assume the transition region is 7 m long and contains 12 solenoids that are 45 cm long, separated by 5 cm, and have adjustable inner radius, radial thickness, and current density. The axial field for each solenoid uses Equation 7.46. The merit function  $f$  for the minimizer compares the desired value of the field at  $N$  locations  $z_i$  from Equation 11.38 with the calculated sum of the fields from all the coils, each with a set of parameters  $a_j$ .

$$f = \sum_{i=1}^N \left[ \left( \sum_{j=1}^{14} B_z(z_i; a_j) \right) - B_z(z_i) \right]^2.$$

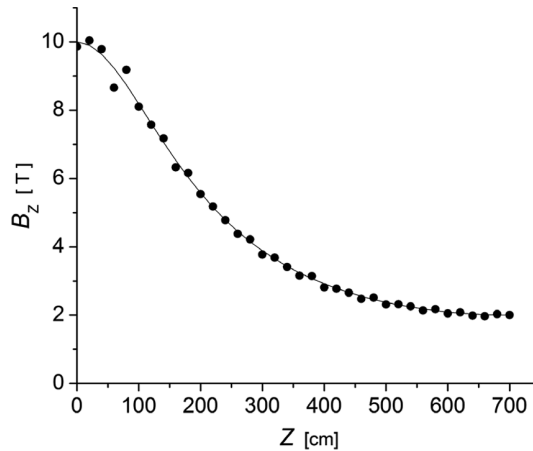


Figure 11.15 The optimized axial field (dots) and the desired field profile (line) in the transition region between two solenoid channels.

The calculation shown here used  $N = 36$ . Minimization of this function used methods that do not require calculation of the derivatives.[27] The initial minimization was done using a simplex algorithm. The most useful parameters to adjust were the current densities and the inner radii of the coils. The axial parameters are severely constrained here by the chosen geometry for the transition region. After a preliminary solution had been found, the Powell direction-set method was used for the final minimization. The optimized axial field is compared with the desired field profile in Figure 11.15.

As a second example of optimization, let us consider the design of the central section of a long dipole magnet with a circular cross-section. Assume that field quality in the dipole aperture is the matter of concern and that we want to minimize the strength of the first four allowed harmonics of the dipole field. We saw in Chapters 4 and 5 that the multipole coefficients depend on the limiting angles of annular conductor blocks. In order to eliminate four multipoles we will need to use at least three blocks. We choose here a conductor design with two radial layers, each of which has two conductor blocks, as shown in Figure 11.16. The contribution to the multipoles from an annular conductor block with constant current density was given in Equations 5.68–5.70. We again use a minimization algorithm, where the merit function is now given by

$$f = \sum_{i=1}^4 w_i \left[ \left( \sum_{j=1}^{16} b_n(n_i; a_j) \right) - \tilde{b}_n(n_i) \right]^2.$$

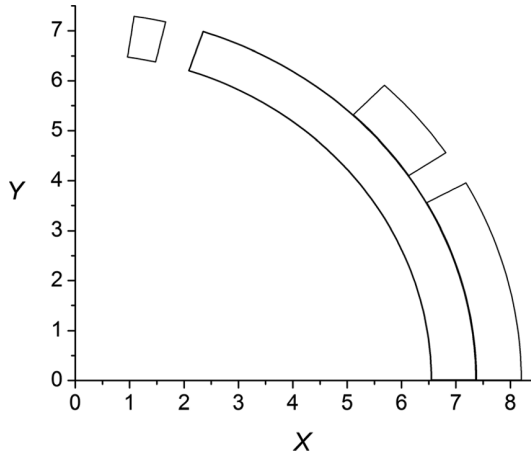


Figure 11.16 Conductor blocks in the first quadrant of a dipole magnet.

The index  $i$  sums over desired multipole orders, the index  $j$  sums over coils, and the normalized multipole ratio is defined as

$$b_n = \frac{B_n [T/m^{n-1}] r_{ref}^{n-1} [m^{n-1}]}{B_1 [T]}.$$

The  $\tilde{b}_n$  factors are the desired values of the multipole ratios, which we take here as 0. The  $a_j$  are the set of parameters that describe conductor block  $j$ . The parameters of the coils in quadrants 2–4 are related to the parameters of the coils in quadrant 1 by the dipole symmetry. For this calculation the adjustable parameters are the end angles of the blocks nearest the midplane and the start and end angles of the second block in each layer. The start angle of the two blocks nearest the midplane are made as close to 0 as possible to maximize the dipole field. The  $w_i$  are weights that determine the importance of satisfying the constraint on multipole  $n_i$ . The reference radius used for the multipole calculations was  $2/3$  of the magnet aperture. After minimization, the allowed multipole ratios  $b_3, b_5, b_7$ , and  $b_9$  have strengths  $\sim 10^{-4}$ .

In the design of actual magnets,[28] a need for high precision field quality may require that allowed multipoles higher than  $b_9$  are also minimized. In addition, the conductor may have to be described in terms of individual turns of the cable separated by the appropriate insulation thickness, instead of the continuous conductor blocks used here. This introduces the additional constraint that there must be an integral number of turns in a conductor block. In addition, if the coils are surrounded by an iron shell, saturation effects, which cause the multipole strength to vary with the excitation current, may have to be taken into account.

## References

- [1] A. Frisiani, G. Molinari & A. Viviani, Introduction, in M. Chari & P. Silvester (eds.), *Finite Elements in Electrical and Magnetic Field Problems*, Wiley, 1980, p. 1–10.
- [2] N. Gershenfeld, *The Nature of Mathematical Modeling*, Cambridge University Press, 1999, p. 86–91.
- [3] K. Binns & P. Lawrenson, *Analysis and Computation of Electric and Magnetic Field Problems*, Pergamon Press, 2nd ed., 1973, p. 246.
- [4] D. Jones, *Methods in Electromagnetic Wave Propagation*, vol. 1, Oxford University Press, 1987, p. 113.
- [5] G. Smith, *Numerical Solution of Partial Differential Equations: Finite Difference Methods*, 2nd ed., Oxford University Press, 1978, p. 216.
- [6] K. Binns & P. Lawrenson, *op. cit.*, p. 268.
- [7] W. Press, S. Teukolsky, W. Vetterling & B. Flannery, *Numerical Recipes in Fortran*, 2nd ed., Cambridge University Press, 1992, p. 117.
- [8] W. Milne, *Numerical Solution of Differential Equations*, Dover, 1970, p. 217.
- [9] G. Parzen & K. Jellett, Computation of high field magnets, *Part. Acc.* 2:169, 1971.
- [10] W. Press, et al., *op. cit.*, p. 857–860.
- [11] K. Binns & P. Lawrenson, *op. cit.*, p. 260–265.
- [12] N. Gershenfeld, *op. cit.*, p. 93–101.
- [13] M. Chari, Finite element solution of magnetic and electric field problems in electrical machines and devices, in M. Chari & P. Silvester (eds.), *Finite Elements in Electrical and Magnetic Field Problems*, Wiley, 1980, p. 87–107.
- [14] R. Gallagher, Shape functions, in M. Chari & P. Silvester (eds.), *ibid.*, p. 49–67.
- [15] P. Silvester & M. Chari, Finite element solution of saturable magnetic field problems, *IEEE Trans. on Power Apparatus and Systems* 89:1642, 1970.
- [16] J. Simkin & C. Trowbridge, Three dimensional nonlinear electromagnetic field computations using scalar potentials, *IEE Proc.* 127:368, 1980.
- [17] J. Simkin & C. Trowbridge, Magnetostatic fields computed using an integral equation derived from Green's theorems, *Proc. Compomag*, Rutherford Appleton Laboratory, Oxford, 1976, p. 5.
- [18] C. Trowbridge, Applications of integral equation methods to the numerical solution of magnetostatic and eddy current problems, in M. Chari & P. Silvester (eds.), *op. cit.*, p. 191–213.
- [19] C. Trowbridge, Progress in magnet design by computer, *Proc. 4th Int. Conf. Magnet Technology*, Brookhaven National Laboratory, 1972, p. 555.
- [20] B. McDonald & A. Wexler, Mutually constrained partial differential and integral equation field formulations, in M. Chari & P. Silvester (eds.), *op. cit.*, p. 161–190.
- [21] M. Newman, C. Trowbridge & L. Turner, *GFUN: an interactive program as an aid to magnet design*, *Proc. 4th Int. Conf. Mag. Tech.*, Brookhaven National Laboratory, 1972, p. 617.
- [22] F. Mingwu, S. Hanguang & W. Jingguo, Some experiences of using integral equation method to calculate magnetostatic fields, *IEEE Trans. Mag.* 21:2185, 1985.
- [23] A. Winslow, Numerical solution of the quasilinear Poisson equation in a nonuniform triangle mesh, *J. Comp. Phys.* 1:149, 1966.
- [24] J. Billen & L. Young, *Poisson-Superfish*, *Los Alamos National Laboratory report LA-UR-96-1834*, 2006, p. 577–596.
- [25] R. Turner, A target field approach to optimal coil design, *J. Phys. D: Appl. Phys.* 19:L147, 1986.

- [26] G. Morgan, Two dimensional, uniform current density, air core coil configurations for the production of specified magnetic fields, Proc. 1969 Part. Accel. Conf., Washington DC, p. 768.
- [27] W. Press, et al., *op. cit.*, p. 402–413.
- [28] E. Bleser, et al., Superconducting magnets for the CBA Project, *Nuc. Instr. Meth. Phys. Res. A* 235:435, 1985.